REPORT OF INVESTIGATIONS 11

GRAVITY SURVEY

of the

RANDALIA MAGNETIC ANOMALY

FAYETTE COUNTY, IOWA

by

Jack L. Gilmore

GRAVITY SURVEY
of the
RANDALIA MAGNETIC ANOMALY
FAYETTE COUNTY, IOWA

by

Jack L. Gilmore

———————

REPORT OF INVESTIGATIONS 11

———————

CONTENTS

ILLUSTRATIONS

GRAVITY SURVEY
of the
RANDALIA MAGNETIC ANOMALY
FAYETTE COUNTY, IOWA

by

Jack L. Gilmore

ABSTRACT

Supplementary gravity data on an anomaly delineated from an aero-magnetic survey of northeastern Iowa is presented in this report. The gravity survey included 240 observation stations located at section corners from central to western Fayette County. Analysis of the simple Bouguer map, residual gravity maps, and gravity profiles suggests that the observed gravity anomalies probably derive primarily from large fault blocks within the Precambrian crystalline complex and related variations in the thickness of superjacent clastic deposits. Interpretations based on magnetic susceptibility indicate that rocks of the basement complex lie at a depth of 2,000 feet (610 m) to 2,700 feet (823 m) below the surface within the study area and vary laterally in composition from basic to acidic. Two areas that exhibit high gravity and magnetic values may warrant exploration for potential mineralization.

INTRODUCTION

Purpose and Scope

The purpose of this investigation was to obtain supplementary data for interpretation of the complex structural and compositional character of the Precambrian basement and the overlying Paleozoic sediments as inferred from aeromagnetic data. The present survey was centered on a prominent magnetic anomaly near the town of Randalia. An outcropping of massive, reniform barite approximately eight miles (13 km) north of Randalia was included in the survey area because of the potential for structural control of mineralization.

Location of Study Area

The study area is located in northeast Iowa and includes most of central and western Fayette County (fig. 1). This is an area of approximately 220 square miles (570 km^2) and is bounded between lat. 42°45' and 43°01'N, and long. 91°42' and 92°04'W.

Previous Work

Between May 8 and May 22, 1966, an airborne magnetometer survey was flown for the Iowa Geological Survey by Aero Service Corporation of Philadelphia, Pennsylvania. Results of this survey revealed a magnetic anomaly roughly 10 miles (16 km) in diameter with an amplitude of 3,300 gammas near the town of Randalia. Depth estimates indicated the source to be about 2,400 feet (730 m) below the surface and therefore probably within the Precambrian basement complex which is believed to occur at
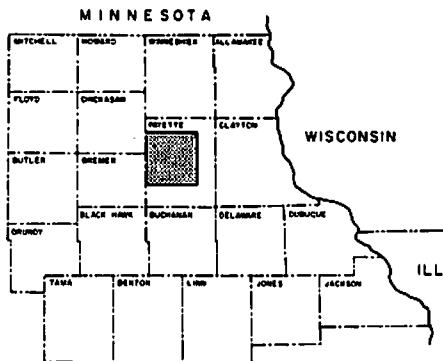

Figure 1. Location of Study Area

approximately the same depth. The source of the anomaly was interpreted by Aero Service Corporation to be one-half mile (0.8 km) wide, three miles (4.8 km) long, and oriented north 60° east-south 60° west by assuming a magnetite content of 10-15 percent in excess of country rock by volume. If the source is considered to be 25-30 percent magnetite in excess of country rock, the width is computed to be one-fourth mile (0.4 km).

The regional magnetic pattern shows a band of intense and high frequency anomalies about 25 miles (40 km) in width trending NNW-SSE from northeastern Howard County to north-central Buchanan County with the Randalia magnetic anomaly lying near the center. This band is interpreted as a "vast trough of lavas and interdigitated clastic rock bounded and controlled by a series of profound longitudinal faults" (Aero Service Corp.). This is in general agreement with gravity interpretations over the Midcontinent Gravity High, the axis of which lies some 75 miles (120 km) west of Randalia. Aero Service Corporation further inferred that regional magnetic highs are expressions of mafic lavas of Middle and Upper Keweenawan age, and areas of reduced intensity reflect accumulations of clastic sediments of a similar age, some of which may be metamorphosed. Linearity, persistence, and abruptness of magnetic gradients are suggestive of major basement faulting. The Randalia anomaly is interpreted as one of a series of intrusive bodies that ascended along the northwest boundary of what may be a zone of imbricated faulting or shearing from Waterloo in Black Hawk County to Wadena in Fayette County. In support of this inference are two magnetic salients suggestive of dikes that extend from the main body in a northwesterly direction (pl. IV).

ACKNOWLEDGEMENTS

GEOLOGY

Bedrock throughout the study area is covered by a veneer of Kansan drift ranging in thickness from 0-250 feet (76.2 m) and averaging about 100 feet (30.5 m). The topography generally is level to gently undulating. The extreme northern boundary and the area around the town of Fayette are cut by major streams to a relief of up to 200 feet (61 m) with bedrock exposed as bluffs at several sites. The Cedar Valley Limestone comprises the bedrock over approximately 90 percent of the area (fig. 2). Subjacent formations down to and including the Maquoketa Formation outcrop in the deeply cut valleys. The Paleozoic sequence is summarized in figure 3.

Fayette County has remained relatively stable since Precambrian time in terms of regional tectonics. Major source areas of clastics, which comprise about 50 percent of the total Paleozoic sequence, include the Wisconsin Arch and the Wisconsin Dome to the east and northeast respectively. Negative features include the Illinois Basin to the southeast and the Forest City Basin to the southwest. Composite structural maps using the top of the Maquoketa Formation and top of the cherty unit within the Galena Formation as datum planes show a rather ill-defined set of anticlinal features trending northwest-southeast throughout the region. Stratigraphic and structural control within the study area are very limited. The nearest deep stratigraphic control site is an exploration hole drilled to a depth of 3,216 feet (980.2 m) by New Jersey Zinc Company in Clayton County (SE 1/4 sec. 8, T. 92N., R. 5W.), about 25 miles (40 km) east-southeast of the town of Randalia. A Precambrian titaniferous dunite was encountered at 1,829 feet (557.5 m) after penetrating about 980 feet (298.7 m) of superjacent clastic sediments of Cambrian age. Core analysis of the basement rock revealed a composition of 28.4 per cent Fe and 10.3 percent TiO_2 (personal correspondence, Frederic Main, New Jersey Zinc Company). In comparison, an oil test located about 30 miles (48 km) southwest of Randalia (NE 1/4 sec. 15, T. 90N., R. 15W., Butler County) penetrated about 1,500 feet (457 m) of fine-grained clastics in the lower portion of the sedimentary sequence without reaching the crystalline basement complex. The lower 1,275 feet (388.6 m) of these clastic sediments are tentatively correlated with the "Red Clastics" (equivalent to the Upper Keweenawan Hinckley-Fond du Lac Formations of northeastern Minnesota). Lithologically, the "Red Clastics" consist of very fine to very coarse, angular to subangular, red, micaceous sandstone with interbedded red and green shales. This unusually thick section of clastics may be related to the belt of mafic lava flows, as interpreted from the aeromagnetic survey, in much the same manner as those flanking the Midcontinent Gravity High farther west where thick clastic deposits are believed to occupy marginal fault-controlled basins.

Generalized   Geologic   Map   of   Fayette   County
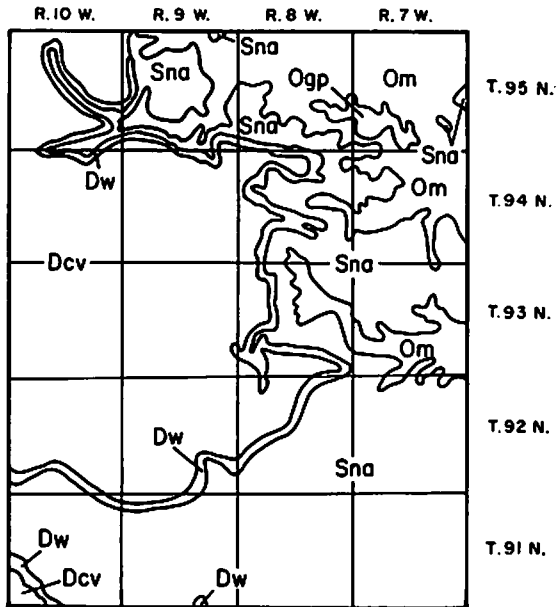
Devonian   System

    | Dcv | Cedar   Valley   Formation

    | Dw | Wapsipinicon   Formation

Silurian   System

    | Sna | Niagaran – Alexandrian   Series

Ordovician   System

    | Om | Maquoketa   Formation

    | Ogp | Galena   and   Decorah – Platteville   Formation

Figure 2.

Generalized   Geologic   Column
of   Fayette   County

	Approximate Thickness	
Quaternary System	(feet)	(meters)
Recent and Pleistocene Series	100	30
Devonian System		
Middle		
Cedar Valley Fm.	25	8
Wapsipinicon Fm.	25	8
Silurian System		
Niagaran Series	40?	12?
Alexandrian Series	40?	12?
Ordovician System		
Cincinnatian Series		
Maquoketa Fm.	250	76
Mohawkian Series		
Galena Fm.	220	67
Decorah-Platteville Fms.	90	27
Chazyan Series		
St. Peter Fm	50	15
Beekmantown Series		
Prairie du Chien Fm.	300	90
Cambrian System		
St. Croix Series		
Trempealeau Group	200	60
Franconia Fm.	150	45
Dresbach Group	500?	150?
Precambrian		
"Red Clastics" . . . . (?)		
Igneous and Metamorphic		

Limestone

Shale

Drift

Dolomite

Sandstone

Chert
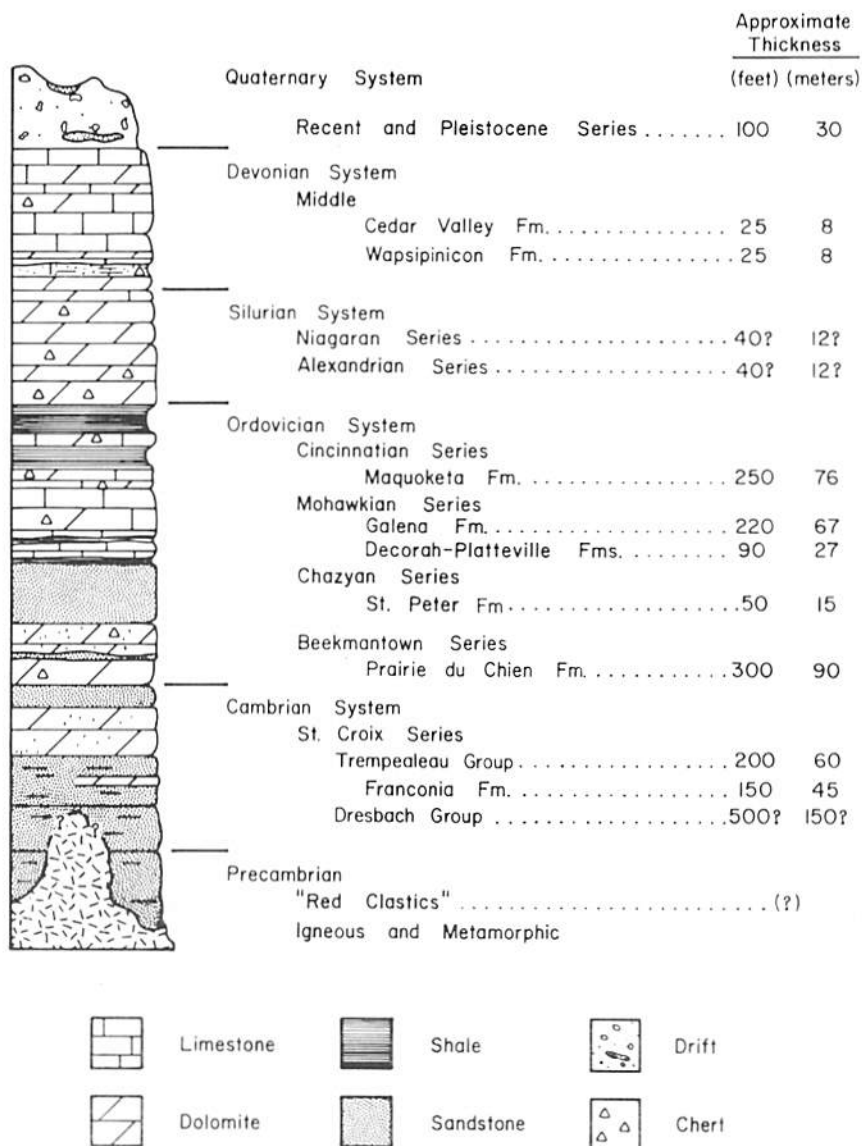
Figure 3.

GRAVITY SURVEY

Gravimetric surveying is one of several geophysical techniques used to assist in the interpretation of subsurface geological phenomena. Many times these investigations reveal sites of mineralization or geologic structures with an economic potential. Differences in the acceleration of gravity are measured with a gravimeter at selected points on the earth's surface and the resulting data is used to generate maps showing lateral variation of gravitational intensity. A gravimeter is an extremely sensitive weighing device capable of detecting differences in gravitational attraction to approximately one part in ten million. The unit of measurement is the milligal (mgal) (1/1,000 gal) and is equal to an acceleration of 0.001 centimeter per second per second.

Field Operations and Techniques

Gravity base station IGS #33 (absolute value 980,377.610 mgals), established at the Clermont Municipal Airport (Hase et al., 1969), was selected as the reference station. Six primary base stations were established around the periphery of the survey area, such that no network station would be more than 10 miles from a primary base station. Observation stations were located at one-mile (1.6093 km) intervals (usually at section corners) and carefully noted to facilitate reoccupation. Where road intersections were not present, distances were measured by automobile odometer, or section line fences were used, to position stations. As 7-1/2 minute topographic coverage was unavailable, a Fayette County Highway and Transportation Map was used as a base map. A total of 1,356 instrument readings were taken at 237 stations. Base stations and stations 1 through 206 were observed during the period between October 1 and October 25, 1968, using a LaCoste-Romberg Model G Geodetic Gravity Meter (no. 59). This instrument can be read to an accuracy of about ±.005 milligals and has a drift rate of less than one milligal per month. Stations 207 through 240 were observed on October 9-10, 1969, using a Worden Gravimeter (no. 751). This instrument can be read to an accuracy of about ±.02 milligals. The LaCoste-Romberg instrument was repeatedly read at individual stations until three consecutive readings differing by less than 0.004 milligals were obtained. Similarly, the Worden Gravimeter was read until two consecutive readings differing by less than 0.2 scale divisions (.02 mgals) were obtained. An average of these consecutive readings at individual stations was taken as the value of the dial reading in subsequent computations.

Loop traverses generally consisted of 15 to 20 station occupations (see appendix) and were closed on base stations in an average time lapse of

4-1/2 hours. Values obtained from Loop no. 10 may, in part, be suspect as it was closed after a longer than normal time lapse while the instrument was affected by microseisms that probably originated from an earthquake in the New Guinea area (measured seven on Richter scale, Univ. of Cal. at Berkeley, October 23, 1968).

Vertical Control

Vertical control was barometrically determined to an accuracy of ± 4 feet (1.2 m) using a Paulin Microaltimeter, Model M-1, calibrated to intervals of one foot. In several instances, elevation profiles along major roads were available and barometric determinations were adjusted accordingly.

Data Reduction

Data reduction was accomplished using a modified computer program designed by Army Map Service for use on the Univac 1108 (Geodetic Memorandum No. 1617, 1967). The program (GRAVAS) was written in Fortran IV to reduce LaCoste-Romberg gravity observations to corrected observed gravity, free-air anomaly and Bouguer anomaly values. The program was modified for use on the IBM-360-65 computer and to accept data from the Worden Gravimeter. Correction values were computed using mean sea level as a datum plane and 2.67 g/cm^3 as the estimated density of crustal strata. Gravity data were also subjected to polynomial trend analysis through the sixth degree surface.

Presentation of Data

The Bouguer gravity map (pl. I) depicts lateral variation of gravitational intensity by comparing corrected observed values to theoretical values. Residual maps (pls. II & III) were generated by a mathematical process that progressively removes regional effects from Bouguer values. In essence, these maps only accentuate features that are present on the Bouguer map. The Aeromagnetic Map-Geophysical Interpretation of Basement Complex (pl. IV) is included for comparative purposes. Four profiles through major features are presented as aids in comparing gravity and magnetic values (figs. 4 & 5). Areas postulated to have the thickest accumulations of clastic sediments and the locations of inferred intrusive bodies and basement faults are shown on plate V.

Precision of Data

The major source of error in this survey is expected to be vertical control. Barometrically determined elevations are considered accurate to within ± 4 feet (1.2 m). Errors of this magnitude introduce a gravity error of 0.38 milligal. Because two or more elevation determinations were averaged for each observation station, a more realistic value of possible gravity error is 0.2 milligal.

Previous experience in determining latitude and longitude from county highway and transportation maps has shown that locations may be in error by as much as 0.2 minute. An error of this magnitude produces a gravity discrepancy of about 0.02 milligals.

An undeterminable error may be present in the Bouguer correction due to variations in crustal density between the observation station and the reference datum (mean sea level). Glacial deposits probably present about a 0.5 g/cm^3 density contrast with the underlying bedrock and therefore constitute a source for a possible error up to 1.5 milligals.

INTERPRETATION

Interpretation of gravity data is ambiguous because a variety of mass distribution models can be postulated to fit the observed data. Consequently, it is essential that one examine and compare as much additional information concerning the survey area as possible in order to make a reasonable interpretation. Woolard (1962), in discussing the gravity field of the central United States, concluded ". . . the key to understanding gravity relations in the midcontinent area appears to be a knowledge of the composition of the crystalline basement. The geologic parameters which can be most effectively related to this are: a) knowledge of the Precambrian structural trends, b) sampling of the basement to determine its composition, and c) consideration of the type and extent of post-Cambrian igneous activity in the area".

Investigations in Illinois (McGinnis, 1966) indicate gravity values are, in part, related to basin formation on a regional and possibly a local scale through isostatic adjustment of fault-bound blocks of the Precambrian crystalline complex. In this respect, higher density blocks sink relative to lighter blocks and in the process accumulate additional mass from the influx of sediments. Thus gravity "highs" would tend to occur over structural "lows" and conversely. This inverse relationship of gravity to regional structure has been pointed out by Henderson and Zietz (1958) in relation to the Cincinnati and Kankakee Arches, by Hinze (1963) in relation to the Michigan Basin, and by Wollard (1962) in referring to the Illinois Basin. This correlation is not apparent in Iowa on a regional scale, but may be valid for local features as discussed later in this section.

Of particular interest is the proposed relationship of Precambrian(?) feldspathic sandstones and Keweenawan mafic lavas. Thiel (1956), working along the Midcontinent Gravity High in northern Minnesota, correlated gravity "highs" with Keweenawan volcanics and gabbro, and gravity "lows" with feldspathic sandstones deposited in fault-controlled marginal basins. Presuming the association to exist farther south, Coons, Woolard, and Hershey (1967) proposed up to 16,000 feet (4877 m) of clastic sediments in marginal fault basins bordering the Midcontinent Gravity High in Iowa where gravity contrasts approach 160 mgals. As mentioned earlier, aeromagnetic data revealed what may be a similar, but subdued, occurrence of mafic flows trending NNW-SSE through northeastern Iowa in a band approximately 25 miles (40 km) wide that includes the subject area of this report. Regional gravity expression of this feature, however, is very weak and poorly defined in comparison to the Midcontinent Gravity High (Woolard & Mack, 1953). This indicates that major marginal faulting and subsequent deposition of very thick clastic sediments have not occurred. However, evidence that some marginal

faulting may be present is the unusually thick section of clastics penetrated in the deep oil test of southeast Butler County referred to earlier. Deviations in the trend of Paleozoic structural contours, generally coincident with the western border of the proposed mafic belt, suggest that some post-Precambrian movement may have taken place. Magnetic data over the proposed mafic lavas show a high degree of linearity in conjunction with high gradients. This is very suggestive of faulting within the basement complex.

Gravity measurements are affected by the density contrast between the glacial drift and the underlying bedrock. Available information shows the glacial drift to range in thickness from 0 to 250 feet (76.2 m), being generally thicker in the west-central part of the study area. Changes in thickness probably are most abrupt along the major drainage courses, particularly along the northern border and in the southeastern portion of the survey area. Density of the glacial drift is estimated to be about 2.2 g/cm^3. A gravitational contrast of 1.9 milligals would be produced by an assumed maximum density contrast of 0.6 g/cm^3 with the underlying bedrock in conjunction with an estimated maximum thickness of 250 feet (76.2 m). As drift commonly is thickest along drainage divides, Bouguer corrections over these areas will tend to overcompensate for elevation changes producing values that may be up to 1.5 milligals lower than predicted.

The Paleozoic sedimentary sequence, with the possible exclusion of lower Cambrian clastics, is not expected to produce significant gravitational contrasts. The study area lies within a region that is believed to have remained tectonically stable since Precambrian time. The previously mentioned anticlinical structures within Paleozoic strata have amplitudes of about 200 feet (61 m) and gradients of about 50 feet per mile (10 m /km). Lithologies are relatively uniform over large areas. Regionally, isopachs of formations above the St. Lawrence dolmite show little change. Disregarding those formations having an erosional contact with recent and glacial deposits, this portion of the section probably shows a change in total thickness of less than 200 feet (61 m). A change of this magnitude, coupled with the greatest probable density contrasts (0.4 g/cm^3), produces a gravity change of only about 1.0 milligal. Information concerning deeper formations is very limited. Cambrian and Precambrian(?) clastics, comprising most of this portion of the section, appear to be highly variable in lithology and thickness. Variability is probably largely dependent upon the configuration of the crystalline basement complex. Lateral displacement of the relatively dense basement rock by clastic sediments probably accounts for a substantial portion of the observed differences in gravitational attraction.

The configuration of the Precambrian crystalline surface is not well

known. Drill data indicate a regional slope to the west-southwest at approximately 30 feet per mile (5.7 m /km) through Fayette County. This agrees well with a general increase in gravity values to the east and northeast. Crystalline rock types within the survey area, as interpreted from aeromagnetic data, range in composition from basic to acidic. The magnetic interpretation is based on the assumption that basic rocks are more likely to contain magnetic minerals (chiefly magnetite) than acidic rocks. Similarly, basic rocks generally are more dense than acidic types and therefore exert a greater force of gravitational attaction. The apparent correlation can, of course, be masked and altered by a variety of influencing factors. As very large volumes of igneous and metamorphic rocks of different densities can be brought into juxtaposition through faulting and intrusion, it is reasonable to assume that the basement complex has a profound effect on gravitational variation. Linearity of gravimetric and magnetic data within the study area is interpreted as evidence of basement faulting. Several areas differing in geophysical expression are thus interpreted as large fault blocks. Relative movement of these proposed fault blocks probably is related, in part, to attaining a state of isostatic equilibrium. To examine the area in terms of isostatic equilibrium, it is necessary to establish the zero free-air anomaly. As elevations are reasonably consistent and average about 1,175 feet (358 m) throughout the study area, the zero free-air anomaly contour line is approximated by the -40 milligal contour line of the Bouguer gravity map (pl. I). Areas having lower values therefore have a tendency to rise isostatically and conversely. Fayette County and much of northeastern Iowa have Bouguer values averaging approximately -25 milligals (Woolard, et al., 1953). This agrees well with the previously noted inverse relationship between gravity and regional structure. Areas exhibiting low gravity values might represent local graben structures. Values lower than the zero free-air value may derive from graben structures that have been carried down with regional subsidence.

Interpretation of gravity features is facilitated by assuming causative bodies to be simple geometric forms which would produce gravity configurations most similar to those actually generated by the observed data. Maximum depth to these proposed bodies can be estimated by simple mathematical formulas. In general, a deeply buried source produces a gravity profile of lower intensity than one which is nearer the surface. Faults usually are inferred from breaks in the trend of isogals and from linear features with high gradients.

The Bouguer map (pl. I) depicts lateral variations of gravitational intensity and ultimately variations in rock density throughout the study area. Specific locations on all maps are referenced to the letter-number grid system shown on each map.

A prominent feature of the Bouguer map is the gravity-low located at I-3. This broad anomaly is bordered on the northeast and southeast by high gradients (4 mgal per mile) which are interpreted as evidence of basement faulting (see pl. V). Bending of the isogals on the south side develops under reduction into the 11 milligal closure seen in the second-degree residual map (pl. II). The feature persists through the sixth-degree surface, but loses magnitude and migrates south and east. High residual gradients on the southwestern flank also are considered to derive from basement faulting. Magnetic data (pl. IV) indicate a north-south fault on the western flank (not shown on map) and a dike of basic composition extending into the area from the southeast. Warping of the isogals in the vicinity of K-7 becomes progressively accentuated through-out the residual series and therefore lends some support to the proposed dike. Circularity of the residual anomaly favors use of a buried vertical cylinder as a model causative body. Using the half-width method (LeRoy, p. 1071), it can be shown that the maximum depth to the top of the cylinder is about 8,500 feet (2.6 km). Presuming the body to extend to the proposed faults, the required density contrast at this depth is calculated to be 0.1 g/cm^3. Magnetic data, however, indicate the basement to lie at a depth of about 2,400 feet (730 m). The required density contrast at this depth is 0.07. g/cm^3. In reference to earlier statements, it should be noted that a thickness of about 2,250 feet (686 m) of clastic sediments presenting a 0.5 g/cm^3 density contrast with crystalline basement might equally well produce the anomaly. From an isostatic viewpoint, the anomalous area is very nearly at equilibrium, in contrast with surrounding areas, and therefore is in accordance with the concept of a graben. Another factor that may be of significance in analyzing this feature is the thickness of the glacial drift. Scanty well data indicate the drift to be thickest over this anomaly and therefore may effect, in part, the low Bouguer values.

Another prominent feature is the elongated gravity high at D-7 on the Bouguer map. Although it is not well defined here, it achieves and maintains a moderately strong expression under trend reduction. Magnetic data at this site suggest a northwest-southeast trending dike of basic composition (pl. IV). Gravity data indicate an elongate body of relatively high density and therefore support the magnetic interpretation. The strong gravity gradients and linearity associated with this anomaly indicate that the proposed intrusive probably was emplaced along a northwest-southeast trending fault.

A gravity low at G-14 (pl. I) is fairly consistent in magnitude and· position under trend analysis. The strong gradient along its northwest border aligns well with the saddle between anomalies D-7 and K-13. This, in addition to the strong gradient and linearity along the southeast side of the I-3 gravity low, is very suggestive of a basement fault that appears to

extend southwest-northeast through most of the study area (see pl. V). The linearity of magnetic patterns supports this interpretation.

The gravity high at K-13 (pl. I) appears to be a southeastern extension of the elongated D-7 feature. This, in addition to the shape of the residual gravity anomaly (pls. II & III), is suggestive of an intrusive body. Depth to the top of the source is calculated as 4,480 feet (1.4 km) by assuming it to be an infinitely long, buried vertical cylinder three miles (4.8 km) in diameter. Further computations show the required density contrast at this depth to be a 0.10 g/cm^3. Magnetic values (pl. IV) indicate the basement crystalline rock here is of basic composition. It is also reasonable to speculate that the feature may be a topographic high on the crystalline basement surrounded by clastic sediments having a density contrast of approximately 0.7 g/cm^3. By further assuming that the causative body lies at a depth of 2,400 feet (730 m), it can be shown that the surrounding clastics must be about 1,800 feet (550 m) thick. If, as the magnetic data suggests, there is a compositional change within the crystalline rock on the northeastern side due to intrusion or faulting, less than 1,800 feet (550 m) of clastics would be expected at G-14.

Magnetic interpretation (pl. IV) indicates a northeast-southwest trending fault, or faults, in the southeastern part of the study area. Gravimetric expression of this proposed feature is weak. A strong gradient based on limited data exists at M-18 (pl. II). This, in addition to a weaker gradient near R-11, supports this aspect of the magnetic interpretation.

Warping of the isogals in the vicinity of K-3 on the Bouguer map (pl. I) develops into a strong gradient in the second (pl. II) and third residuals. Magnetic contours also exhibit a strong gradient and good lineation in about the same area. A series of elongate low amplitude features develop under further trend analysis suggesting the possibility of several closely spaced faults trending northwest-southeast through the area. A local structural high in the Paleozoic section southwest of this location, indicating minor faulting or folding, tends to support this interpretation.

The peak magnetic value of the Randalia anomaly is at M-10 (pl. IV). Gravity values here are intermediate in relation to the total study area and gradients are low. Under trend analysis the area actually develops about a 2.0 milligal negative closure. A moderately strong gravity gradient on the northeastern flank could be interpreted as a northwest-southeast trending fault separating it from the anomaly at K-13 (pl. V). A relatively thick section of subsequent clastic deposits might explain the weak gravity expression.

SUMMARY AND CONCLUSIONS

Gravity data aid in the interpretation of the subsurface geology in the area of the Randalia magnetic anomaly. Extant well data provide only limited information concerning such important parameters as thickness of glacial deposits, rock density, local structure, and depth and composition of the Precambrian basement complex.

In general, gravity data exhibit good linearity and an absence of tight closures. These characteristics are presumed to derive primarily from compositional variations and structural features within lower Cambrian and/or Precambrian rocks. Linear elements are interpreted as faults. These characteristically separate areas with different magnetic and/or gravimetric expression. Apparent disagreement between magnetic and gravity data may be related to clastic deposits in grabens similar to those proposed on the Midcontinent Gravity High.

Features most interesting in terms of economic potential include the gravity highs at K-13 and D-7. Both of these anomalies exhibit a high magnetic susceptibility and consequently a greater probability of containing significant deposits of magnetic ores (chiefly magnetite). Proposed faults in proximity to these features also warrant closer examination as potential sites of mineralization.

Two outcroppings of barite are present along the upper reaches of Turner Creek near the northern edge of the study area (Koch, 1976; manuscript in preparation). The mineral occurs in the Wapsipinicon formation (middle Devonian) as massive reniform barite up to 1.5 feet (.46 m) thick in collapse-related(?) openings, as fracture fillings in limestone micrite, and as radially divergent crystals intergrown with calcite within a limestone breccia. Barite might have precipitated from low-temperature solutions of magmatic origin related to the Randalia magnetic anomaly or associated features as delineated by gravity data.

Figure 4.

Gravity and Magnetic Profile A-A'

Bouguer (mgals) ....
Magnetic (gammas) --------
2nd° residual (mgals) ———
5th° residual (mgals) —·—·—

Gravity and Magnetic Profile B-B'

Bouguer (mgals) ....
Magnetic (gammas) --------
2nd° residual (mgals) ———
5th° residual (mgals) —·—·—

RANDALIA MAGNETIC ANOMALY

16
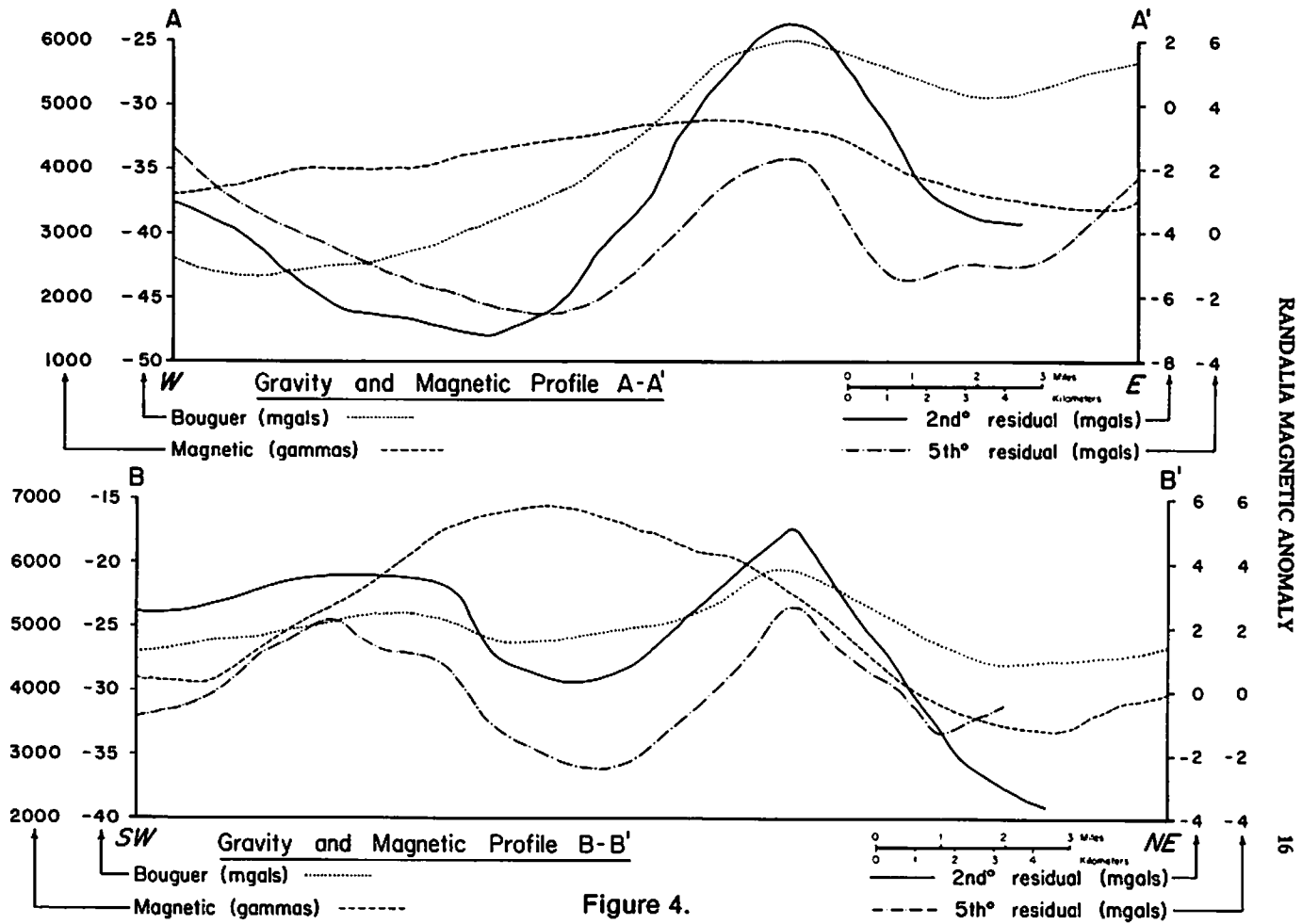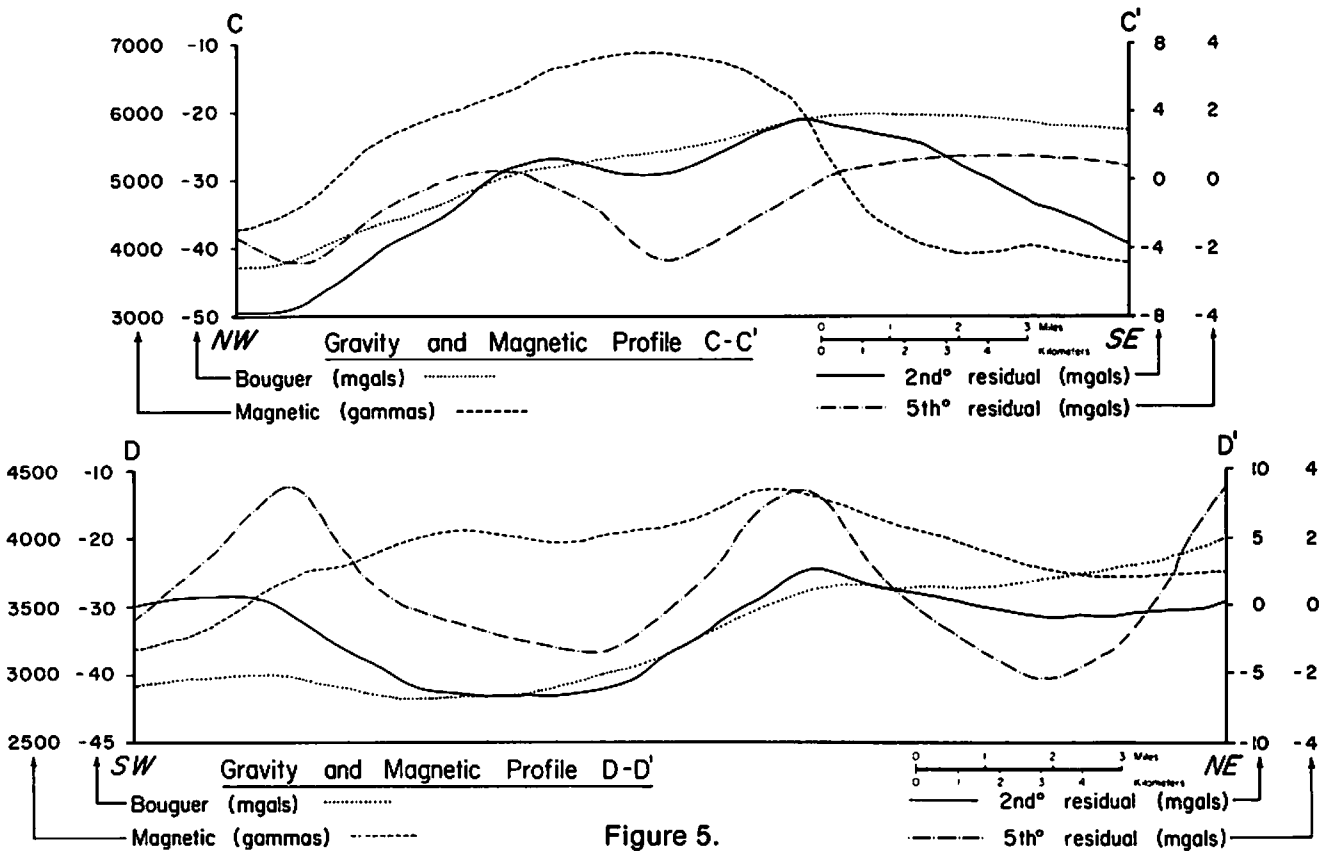
Figure 5.

SELECTED REFERENCES

COONS, R. L., WOOLARD, G. P., and HERSHEY, G., *1967,* Structural significance and analysis of Midcontinent Gravity High: Amer. Assoc. Petrol. Geol., v. 51, p. 2381-2399.

DOBRIN, M. B., *1952,* Introduction to geophysical prospecting: New York, McGraw-Hill, p. 85-102.

GRANT, F. S., and WEST, G. F., *1965,* Interpretation theory in applied geophysics: New York, McGraw-Hill, p. 189-305.

HASE, D. H., CAMPBELL, R. C., and VAN ECK, O. J., *1969,* Iowa gravity base station network: Iowa Geological Survey, Rept. of Inv. no. 8.

HENDERSON, J. R., and ZIETZ, ISIDORE, *1958,* Interpretation of an aeromagnetic survey of Indiana: U. S. Geol. Survey Prof. Paper 316-B, 36 p.

HINZE, W. J., *1963,* Regional gravity and magnetic anomaly maps of the southern peninsula of Michigan: Michigan Dept. Conserv., Michigan Geol. Survey Rept. Inv. 1, 26 p.

IOWA GEOLOGICAL SURVEY, *1968,* Preliminary interpretation report, airborne magnetometer survey of northeastern Iowa: Open file rept., 26 p.

KING, E., and ZIETZ, I., *1971,* Aeromagnetic study of the Midcontinent Gravity High of central United States: Geol. Soc. Amer. Bull., v. 82., p. 2187-2208.

LeROY, L. W., *1951,* Subsurface geologic methods: Denver, Colo.: Peerless Printing Co., p. 1042-1084.

LIDIAK, E. G., MARVIN, R. F., THOMAS H. H. and BASS, S. S., *1966,* Geochronology of the midcontinent region no. 3: Jour. Geophy. Res., v. 71, p. 5427-5438.

McGINNIS, L. D., *1966,* Crustal tectonics and Precambrian basement in northeastern Illinois: Illinois Geological Survey, Rept. of Inv. no. 219, 29 p.

MUEHLBERGER, W. R., DENISON, R. E., and LIDIAK, E. G., *1967,* Basement rocks in the continental interior of the United States: Amer. Assco. Petrol. Geol. Bull., v 51, p. 2351-2380.

NETTLETON, L. L., *1940,* Geophysical prospecting for oil: New York, McGraw-Hill, 444 p.

. . . . , *1942,* Gravity and magnetic calculations: Geophy., v. 7, p. 293-310.

PARASNIS, D. S., *1966,* Mining Geophysics: New York, Elsevier Publishing Co., p. 208-261.

RUDMAN, A. J., SUMMERSON, C. H., and HINZE, W. J., *1965*, Geology of basement in midwestern United States: Amer. Assoc. Petrol. Geol. Bull., v. 49, no. 7, p. 894-904.

SUTTERLIN, P. G., and BRIGHAM, R. J., *1967*, Trend surface analysis, a new look at old data: 6th Ann. Conf. of Ontario Petrol. Inst., Univ. of Western Ontario Tech. Rept., 24 p.

THIEL, E. C., *1956*, Correlation of gravity anomalies with Keweenawan geology of Wisconsin and Minnesota: Geol. Soc. Amer. Bull., v. 67, p. 1079-1100.

U. S. ARMY MAP SERVICE, Dept. of Geodesy, *1967*, A computer program to reduce land gravity observations: U. S. Army Geodetic Memorandum No. 1617, 64 p.

WOOLARD, G. P., *1962*, The determination of gravity from elevation and geologic data: Univ. Wisconsin Geophys. and Polar Research Center, Research Rept. Ser. 62-9, 256 p.

. . . ., and MACK, J., *1953*, Gravity map of Iowa: Iowa Geological Survey, unpublished.

YOHO, W. H., *1967*, Preliminary report on basement complex rocks in Iowa; Iowa Geological Survey, Rept. of Inv. no. 3, 19 p.

APPENDIX I
Gravity Station Traverse Loops

Loop Number	Gravity Stations
1	1001 through 1007
2	1002, 9 through 14
3	1002, 16 through 41
4	1007, 43 through 54
5	1007, 55 through 69
6	1007, 70 through 90
7	1006, 91 through 104
8	1003, 105 through 129
9	1004, 130 through 153
10	1007, 154 through 182
11	1007, 183 through 190
12	1005, 191 through 206
13	1002, 207 through 224
14	1002, 225 through 240

BASIC GRAVITY DATA

Sta. No.	Lat. North	Long. East	Elev. (meters)	Observed Gravity	Free Air Anomaly	Bouguer Anomaly	Residual Trend Surfaces					
							First	Second	Third	Fourth	Fifth	Sixth
1001	42 58.9	91 39.2	264.9	980377.610	11.974	-17.678						
1002	42 57.9	91 48.3	345.9	980354.261	15.142	-23.586	0.08	-0.86	-0.04	0.20	0.30	1.03
1003	42 57.9	92 4.9	362.7	980333.894	- 0.053	-40.658	-1.64	2.04	0.25	-1.69	0.87	0.43
1004	42 50.9	92 4.9	325.5	980330.350	- 4.570	-41.011	-4.31	0.37	2.74	0.64	-1.13	-0.41
1005	42 42.9	92 4.9	319.1	980330.722	5.823	-29.902	-4.66	-8.88	0.49	1.56	-0.04	
1006	42 43.0	91 48.2	364.5	980328.643	17.607	-23.203	4.01	-2.73	2.07	-0.11	0.41	
1007	42 50.7	91 53.0	340.2	980343.126	13.020	-25.060	0.48	1.66	0.33	0.78	-0.91	-0.47
9	42 57.8	91 49.5	351.1	980352.123	14.753	-24.555	0.18	-1.20	-0.14	-1.24	-1.55	-0.88
10	42 57.8	91 50.7	366.4	980349.202	16.534	-24.480	1.36	-0.38	0.89	-1.02	-1.67	-1.25
11	42 57.8	91 51.9	360.9	980350.968	16.607	-23.793	3.16	1.21	2.63	0.15	-0.48	-0.44
12	42 57.8	91 53.1	366.4	980349.098	16.429	-24.585	3.45	1.41	2.93	0.16	-0.24	-0.60
13	42 57.8	91 54.2	363.6	980347.891	14.377	-26.330	2.82	0.79	2.35	-0.42	-0.58	-1.26
14	42 57.8	91 55.4	353.3	980348.748	12.036	-27.511	2.72	0.84	2.37	-0.12	-0.21	-1.06
16	42 57.0	91 48.2	339.9	980354.242	14.592	-23.453	-0.13	0.03	0.73	0.47	2.05	2.09
17	42 57.0	91 49.4	343.2	980352.094	13.479	-24.942	-0.48	-0.85	0.16	-1.02	-0.67	-0.89
18	42 56.9	91 50.6	357.8	980349.224	15.272	-24.786	0.76	0.05	1.31	-0.60	-0.82	-1.37
19	42 57.0	91 51.9	365.8	980349.218	17.562	-23.384	3.28	2.30	3.80	1.36	1.01	0.16
20	42 57.0	91 53.0	376.7	980346.133	17.863	-24.311	3.44	2.33	4.00	1.34	1.16	0.08
21	42 56.9	91 54.2	363.0	980347.727	15.374	-25.264	3.58	2.48	4.29	1.67	1.77	0.58
22	42 56.9	91 55.4	362.4	980346.522	13.981	-26.589	3.33	2.36	4.25	1.95	2.25	1.11
23	42 56.1	91 55.4	354.8	980345.493	11.801	-27.916	1.72	1.49	3.46	1.68	2.41	1.42
24	42 56.0	91 54.2	360.3	980346.630	14.781	-25.551	2.98	2.67	4.46	2.35	2.75	1.51

Sta. No.	Lat. North	Long. East	Elev. (meters)	Observed Gravity	Free Air Anomaly	Bouguer Anomaly	Residual Trend Surface					
							First	Second	Third	Fourth	Fifth	Sixth
25	42 56.1	91 53.0	363.3	980348.501	17.443	-23.230	4.22	3.93	5.52	3.35	3.38	2.04
26	42 56.1	91 51.9	373.4	980346.293	18.338	-23.461	2.90	2.77	4.11	2.16	2.00	0.71
27	42 56.1	91 50.7	357.8	980347.387	14.636	-25.423	-0.15	-0.02	1.05	-0.44	-0.43	-1.54
28	42 56.1	91 49.4	355.4	980346.648	13.144	-26.641	-2.49	-1.94	-1.18	-1.96	-1.22	-2.08
29	42 56.1	91 48.2	339.9	980350.786	12.486	-25.559	-2.50	-1.42	-0.97	-0.94	1.15	0.57
30	42 55.2	91 48.3	349.0	980345.359	11.230	-27.839	-5.06	-3.24	-3.17	-2.59	-0.42	-1.27
31	42 55.2	91 49.4	351.7	980343.970	10.688	-28.688	-4.82	-3.57	-3.16	-3.35	-2.59	-3.66
32	42 55.2	91 50.6	364.5	980342.339	13.007	-27.803	-2.82	-2.00	-1.28	-2.12	-2.13	-3.36
33	42 55.2	91 53.0	352.7	980347.783	14.783	-24.695	2.48	2.81	4.14	2.62	2.69	1.53
34	42 55.2	91 54.2	357.8	980343.725	12.324	-27.735	0.54	0.81	2.40	0.94	1.48	0.57
35	42 55.2	91 55.4	361.8	980339.332	9.153	-31.349	-2.00	-1.67	0.16	-0.99	0.03	-0.51
36	42 54.3	91 55.4	348.1	980338.561	5.501	-33.466	-4.40	-3.64	-2.13	-2.63	-1.53	-1.45
37	42 54.4	91 54.2	349.9	980343.013	10.367	-28.804	-0.84	-0.10	1.10	0.33	0.79	0.45
38	42 54.4	91 53.0	353.9	980345.432	14.008	-25.606	1.26	2.09	2.99	2.19	2.07	1.39
39	42 54.3	91 51.8	357.2	980345.757	15.518	-24.472	1.29	2.34	2.92	2.35	1.91	1.02
40	42 54.3	91 50.6	354.8	980343.937	12.945	-26.772	-2.09	-0.72	-0.46	-0.58	-0.90	-1.87
41	42 54.4	91 48.2	349.6	980343.257	10.516	-28.621	-6.15	-3.72	-4.10	-2.89	-1.08	-1.85
43	42 52.5	91 53.0	340.5	980346.639	13.927	-24.187	2.07	3.40	3.19	3.44	2.46	2.80
44	42 52.6	91 54.2	343.8	980341.320	9.493	-28.996	-1.63	-0.46	-0.34	-0.14	-0.38	0.29
45	42 52.6	91 55.4	340.2	980336.709	3.753	-34.327	-5.86	-4.71	-4.25	-3.89	-3.29	-2.28
46	42 53.4	91 55.4	342.6	980337.471	4.068	-34.284	-5.53	-4.49	-3.48	-3.43	-2.50	-1.83
47	42 55.4	91 54.2	356.0	980339.974	7.708	-32.146	-4.49	-3.45	-2.76	-2.94	-2.77	-2.50
48	42 53.4	91 53.0	349.9	980345.283	14.137	-25.035	1.50	2.68	3.02	2.87	2.34	2.25
49	42 53.4	91 51.9	343.2	980348.209	14.994	-23.427	2.02	3.44	3.45	3.55	2.63	2.28

Sta. No.	Lat. North	Long. East	Elev. (meters)	Observed Gravity	Free Air Anomaly	Bouguer Anomaly	First	Second	Third	Fourth	Fifth	Sixth
50	42 53.4	91 50.7	349.3	980346.420	15.085	-24.018	0.34	2.12	1.83	2.36	1.52	1.02
51	42 53.4	91 48.2	334.1	980345.526	9.489	-27.908	-6.08	-2.98	3.93	-2.01	-0.39	-0.77
52	42 52.5	91 48.5	338.0	980344.285	10.821	-27.019	-4.92	-1.91	-3.18	-1.25	-1.22	-1.23
53	42 52.5	91 50.7	347.8	980347.322	16.867	-22.065	2.00	4.00	3.19	4.13	2.74	2.68
54	42 52.5	91 51.8	346.6	980347.748	16.917	-21.879	3.27	4.88	4.34	4.86	3.44	3.52
55	42 50.8	91 51.9	330.4	980347.609	14.344	-22.644	1.93	3.43	1.91	2.59	0.51	0.81
56	42 50.7	91 50.7	334.4	980348.653	16.760	-20.671	2.80	4.75	3.04	4.09	2.03	2.30
57	42 50.8	91 49.5	331.0	980346.670	13.519	-23.463	-1.09	1.43	-0.41	1.03	-0.57	-0.21
58	42 51.6	91 49.2	334.7	980346.535	13.387	-24.079	-1.68	1.07	-0.49	1.23	0.08	0.35
59	42 51.5	91 50.8	333.8	980350.948	17.667	-19.696	4.14	6.14	4.79	5.87	3.94	4.19
60	42 51.7	91 51.9	346.6	980346.995	17.364	-21.432	3.44	5.07	4.03	4.74	2.90	3.22
61	42 51.7	91 53.0	337.7	980346.214	13.856	-23.951	2.02	3.36	2.60	3.04	1.65	2.17
62	42 51.7	91 54.2	344.4	980341.363	11.074	-27.484	-0.42	0.73	0.28	0.64	-0.02	0.77
63	42 51.7	91 55.4	333.5	980339.462	5.787	-31.542	-3.38	-2.28	-2.41	-1.96	-1.76	-0.71
64	42 50.8	91 55.4	338.3	980340.173	9.353	-28.522	-0.64	0.25	-0.44	-0.10	-0.25	0.57
65	42 50.8	91 54.2	340.8	980341.417	11.349	-26.799	-0.02	0.95	-0.06	0.25	-0.73	-0.08
66	42 49.9	91 55.4	337.4	980340.428	10.675	-27.097	0.49	1.03	-0.20	-0.12	-0.50	-0.13
67	42 49.9	91 53.0	327.1	980344.275	11.324	-25.288	0.11	0.98	-0.73	-0.50	-2.21	-2.06
68	42 49.9	91 51.9	320.7	980347.882	12.957	-22.939	1.35	2.58	0.71	1.17	-0.84	-0.77
69	42 49.9	91 50.7	323.4	980348.744	14.665	-21.537	1.65	3.34	1.36	2.11	0.19	0.29
70	42 49.0	91 55.4	345.6	980338.389	12.525	-26.168	1.11	1.12	-0.55	-0.81	-1.26	-1.37
71	42 49.0	91 54.2	331.0	980342.093	11.715	-25.340	0.84	0.98	-0.88	-1.10	-2.12	-2.29
72	42 49.0	91 53.0	324.9	980345.370	13.112	-23.262	1.82	2.22	0.21	0.12	-1.31	-1.56
73	42 49.1	91 51.9	328.6	980346.883	15.603	-21.180	2.82	3.60	1.53	1.63	0.06	-0.22

Column group header spanning First–Sixth: **Residual Trend Surfaces**

Sta. No.	Lat. North	Long. East	Elev. (meters)	Observed Gravity	Free Air Anomaly	Bouguer Anomaly	Residual Trend Surfaces					
							First	Second	Third	Fourth	Fifth	Sixth
74	42 49.0	91 50.7	342.9	980343.644	16.934	−21.452	1.45	2.73	0.66	0.96	−0.42	−0.61
75	42 49.0	91 49.5	336.2	980343.399	14.620	−23.016	−1.22	0.67	−1.32	−0.89	−1.79	−1.74
76	42 49.0	91 48.3	326.1	980346.307	14.425	−22.085	−1.39	1.25	−0.56	−0.18	−0.53	−0.11
77	42 48.2	91 48.3	332.8	980344.617	16.003	−21.257	−0.85	1.28	−0.13	−0.66	−0.10	0.18
78	42 48.2	91 49.5	349.9	980340.742	17.394	−21.777	−0.29	1.07	−0.65	−0.90	−0.78	−0.95
79	42 48.2	91 50.7	354.8	980340.248	18.406	−21.312	1.28	1.98	0.04	−0.16	−0.56	−1.05
80	42 48.2	91 51.9	341.1	980343.599	17.524	−20.658	3.03	3.22	1.15	0.89	0.11	−0.50
81	42 48.2	91 53.0	354.2	980346.120		(erroneous values--not employed in mapping)						
82	42 48.2	91 54.2	340.8	980341.472	15.304	−22.844	3.03	2.53	0.46	−0.01	−0.72	−1.21
83	42 48.2	91 55.4	333.5	980342.631	14.205	−23.123	3.85	3.18	1.23	0.70	0.34	−0.09
84	42 47.3	91 55.4	340.8	980341.018	16.199	−21.949	4.72	3.17	1.13	0.56	0.36	−0.07
85	42 47.3	91 54.2	349.0	980340.346	18.067	−21.002	4.57	3.23	1.17	0.65	0.38	−0.15
86	42 47.3	91 53.0	328.6	980344.908	16.327	−20.456	4.03	3.00	1.02	0.53	0.40	−0.25
87	42 47.3	91 51.8	345.3	980341.813	18.405	−20.254	3.13	2.53	0.73	0.23	0.50	−0.21
88	42 47.3	91 50.7	349.0	980341.032	18.752	−20.317	1.96	1.93	0.40	−0.21	0.66	0.06
89	42 47.3	91 49.4	354.8	980339.060	18.568	−21.150	0.02	0.69	−0.47	−1.36	0.13	−0.13
90	42 47.3	91 48.3	335.9	980342.219	15.895	−21.707	−1.61	−0.14	−0.82	−2.28	−0.45	−0.21
91	42 46.4	91 48.3	356.9	980336.441	17.956	−22.000	−2.21	−1.58	−1.16	−3.40	−0.17	0.26
92	42 46.4	91 49.4	359.1	980336.220	18.393	−21.802	−0.91	−1.12	−1.38	−2.68	0.23	0.12
93	42 46.4	91 50.6	348.7	980338.929	17.905	−21.130	0.86	−0.06	−0.87	−1.60	0.53	0.11
94	42 46.4	91 51.8	335.9	980341.587	16.612	−20.989	2.09	0.57	−0.66	−1.06	0.22	−0.26
95	42 46.4	91 53.0	335.6	980341.095	16.027	−21.540	2.56	0.58	−0.95	−1.17	−0.58	−0.94
96	42 46.4	91 54.2	358.8	980337.484	19.564	−20.597	4.65	2.29	0.54	0.41	0.44	0.28
97	42 46.4	91 55.3	362.1	980336.136	19.250	−21.287	5.05	2.47	0.60	0.48	0.24	0.22

Sta. No.	Lat. North	Long. East	Elev. (meters)	Observed Gravity	Free Air Anomaly	Bouguer Anomaly	First	Second	Third	Fourth	Fifth	Sixth
									Residual Trend Surfaces			
98	42 45.5	91 55.3	356.3	980336.605	19.282	-20.306	5.41	1.63	0.25	1.32	0.44	1.09
99	42 45.5	91 54.2	339.5	980339.140	16.644	-21.367	3.54	0.03	-1.09	-0.13	-0.34	0.15
100	42 45.5	91 53.0	348.1	980336.714	16.851	-22.115	1.71	-1.40	-2.16	-1.47	-0.73	-0.49
101	42 45.5	91 51.8	338.9	980338.413	15.728	-22.215	0.56	-2.05	-2.35	-2.07	-0.22	-0.16
102	42 45.6	91 50.6	356.3	980334.995	17.521	-22.367	-0.69	-2.67	-2.36	-2.70	0.35	0.40
103	42 45.6	91 49.4	354.2	980335.182	17.050	-22.599	-2.01	-3.24	-2.20	-3.47	0.53	0.83
104	42 45.6	91 48.3	349.9	980336.174	16.725	-22.446	-2.97	-3.31	-1.39	-4.04	0.24	1.08
105	42 57.9	92 3.7	345.3	980344.550			(erroneous values--not employed in mapping)					
106	42 57.9	92 2.5	337.7	980341.479	- 0.180	-37.986	-1.17	0.40	0.05	0.41	-2.56	-2.14
107	42 57.9	92 1.3	331.3	980345.653	2.019	-35.071	0.65	1.35	1.55	1.95	-1.14	-0.83
108	42 57.9	92 0.1	338.9	980347.861	6.579	-31.364	3.26	3.20	3.84	3.86	1.40	1.40
109	42 57.8	91 59.0	344.7	980349.398	10.053	-28.539	4.99	4.30	5.29	4.69	3.10	2.74
110	42 57.8	91 57.8	337.1	980352.179	10.483	-27.256	5.16	3.97	5.25	3.93	3.15	2.48
111	42 57.8	91 56.6	335.9	980351.911	9.838	-27.764	3.54	1.96	3.42	1.43	1.16	0.30
112	42 56.9	91 56.6	339.9	980350.463	10.963	-27.083	3.93	3.21	5.13	3.39	3.67	2.75
113	42 56.9	91 57.8	346.3	980347.088	9.563	-29.199	2.92	2.57	4.45	3.44	3.37	2.78
114	42 57.0	91 58.9	350.2	980343.219	6.766	-32.439	0.79	0.92	2.69	2.46	1.74	1.52
115	42 57.0	92 0.1	352.4	980338.944	3.150	-36.295	-1.96	-1.23	0.34	0.82	-0.72	-0.62
116	42 57.0	92 1.3	354.5	980336.269	1.133	-38.550	-3.11	-1.66	-0.37	0.60	-1.67	-1.41
117	42 57.0	92 2.5	346.6	980336.327	- 1.254	-40.050	-3.53	-1.22	-0.29	0.75	-1.69	-1.54
118	42 56.2	92 2.5	360.9	980330.703	- 1.258	-41.658	-5.43	-2.55	-0.73	1.00	-0.63	-0.66
119	42 56.1	92 1.3	369.7	980330.048	0.965	-40.424	-5.28	-3.23	-1.21	0.38	-0.86	-0.54
120	42 56.1	92 0.1	362.4	980333.588	2.248	-38.323	-4.28	-2.92	-0.79	0.28	-0.20	0.14

Sta. No.	Lat. North	Long. East	Elev. (meters)	Observed Gravity	Free Air Anomaly	Bouguer Anomaly	Residual Trend Surfaces					
							First	Second	Third	Fourth	Fifth	Sixth
121	42 56.1	91 59.0	364.5	980335.288	4.605	-36.204	-3.25	-2.48	-0.30	0.03	0.27	0.39
122	42 56.1	91 57.8	357.5	980339.382	6.536	-33.488	-1.64	-1.32	0.85	0.39	1.13	0.91
123	42 56.1	91 56.6	353.0	980343.509	9.253	-30.260	0.47	0.46	2.56	1.35	2.23	1.60
124	42 55.2	91 56.6	352.4	980338.246	5.151	-34.293	-3.84	-3.32	-1.28	-1.87	-0.51	-0.61
125	42 55.2	91 57.8	348.7	980336.517	2.294	-36.741	-5.19	-4.36	-2.16	-2.04	-0.63	-0.34
126	42 55.3	91 59.0	371.2	980329.588	2.174	-39.385	-6.72	-5.46	-3.14	-2.23	-1.15	-0.58
127	42 55.3	92 0.1	367.6	980329.094	0.552	-40.598	-6.86	-5.06	-2.66	-1.05	-0.58	0.05
128	42 55.3	92 1.3	362.1	980329.315	- 0.919	-41.456	-6.60	-4.13	-1.73	0.40	0.07	0.47
129	42 55.3	92 2.5	365.5	980327.408	- 1.792	-42.703	-6.75	-3.48	-1.12	1.15	0.27	0.12
130	42 50.8	92 2.5	338.6	980332.054	1.328	-36.581	-2.13	0.86	2.44	3.17	2.92	1.38
131	42 51.7	92 2.5	341.1	980331.543	0.219	-37.963	-3.23	0.13	2.17	3.85	3.81	2.52
132	42 52.6	92 2.5	343.8	980329.103	- 2.724	-41.213	-6.19	-2.60	-0.20	2.13	2.22	1.30
133	42 53.5	92 2.5	353.9	980326.983	- 3.091	-42.705	-7.39	-3.74	-1.12	1.54	1.59	1.01
134	42 54.4	92 2.5	363.0	980326.052	- 2.551	-43.189	-7.55	-4.01	-1.39	1.24	0.96	0.65
135	42 54.4	92 1.3	362.1	980326.504	- 2.380	-42.916	-8.36	-5.59	-3.05	-0.52	-0.11	0.31
136	42 53.5	92 1.3	371.9	980322.916	- 1.609	-43.237	-9.00	-6.09	-3.67	-1.02	-0.17	0.08
137	42 52.6	92 1.3	365.2	980323.705	- 1.539	-42.416	-8.49	-5.62	-3.50	-1.06	-0.09	-0.18
138	42 51.7	92 1.3	355.1	980326.686	- 0.312	-40.063	-6.42	-3.74	-2.06	-0.13	0.74	0.14
139	42 50.8	92 1.3	357.2	980329.155	4.166	-35.824	-2.47	-0.13	1.03	2.19	2.83	1.70
140	42 50.8	92 0.1	360.9	980326.220	2.359	-38.041	-5.78	-3.98	-3.21	-1.98	-0.70	-1.12
141	42 51.7	92 0.1	349.3	980327.185	- 1.599	-40.703	-8.16	-6.04	-4.72	-2.90	-1.37	-1.19
142	42 52.6	92 0.1	360.9	980324.312	- 2.249	-42.649	-9.81	-7.53	-5.72	-3.54	-1.89	-1.24
143	42 53.9	92 0.1	346.9	980329.167	- 3.670	-42.500	-9.23	-6.99	-4.68	-2.48	-1.05	-0.14
144	42 54.4	91 59.0	357.2	980329.739	- 0.650	-40.640	-8.27	-6.68	-4.44	-3.07	-1.41	-0.45
145	42 53.4	91 59.0	356.3	980326.871	- 2.300	-42.188	-10.14	-8.35	-6.41	-4.73	-2.76	-1.56

Sta. No.	Lat. North	Long. East	Elev. (meters)	Observed Gravity	Free Air Anomaly	Bouguer Anomaly	Residual Trend Surface					
							First	Second	Third	Fourth	Fifth	Sixth
146	42 52.6	91 59.0	342.6	980329.577	- 2.627	-40.979	-9.23	-7.41	-5.92	-4.20	-2.23	-1.10
147	42 51.7	91 59.0	344.7	980329.265	- 0.931	-39.522	-8.06	-6.38	-5.42	-3.92	-2.15	-1.37
148	42 50.8	91 59.0	345.3	980330.277	1.620	-37.039	-5.89	-4.51	-4.14	-3.10	-1.63	-1.42
149	42 50.8	91 57.8	342.6	980334.470	4.966	-33.386	-3.33	-2.24	-2.26	-1.49	-0.26	0.39
150	42 51.7	91 57.8	345.6	980333.278	3.365	-35.329	-4.97	-3.61	-3.00	-1.92	-0.33	0.79
151	42 52.6	91 57.8	348.4	980331.785	1.368	-37.633	-6.99	-5.52	-4.36	-3.18	-1.33	0.00
152	42 53.4	91 57.8	355.1	980329.722	0.174	-39.577	-8.64	-7.22	-5.58	-4.54	-2.57	-1.35
153	42 54.4	91 57.8	356.3	980331.029	0.358	-39.530	-8.27	-7.09	-5.06	-4.42	-2.61	-1.79
154	42 50.8	91 56.6	335.6	980339.398	7.732	-29.836	0.86	0.08	-0.28	0.24	0.89	1.74
155	42 51.7	91 56.6	356.6	980332.506	5.979	-33.944	-4.68	-3.51	-3.26	-2.55	-1.53	-0.34
156	42 52.6	91 56.6	344.4	980333.279	1.639	-36.918	-7.36	-6.11	-5.29	-4.59	-3.23	-1.98
157	42 53.4	91 56.6	340.8	980334.787	0.819	-37.328	-7.48	-6.31	-4.97	-4.51	-2.93	-1.92
158	42 54.4	91 56.6	347.2	980335.294	1.801	-37.063	-6.90	-6.00	-4.21	-4.24	-2.64	-2.18
159	42 49.9	91 56.6	342.0	980339.171	10.829	-27.455	1.21	1.76	0.82	0.98	1.33	1.64
160	42 49.9	91 57.8	345.3	980335.394	8.087	-30.573	-0.81	-0.14	-0.73	-0.43	0.47	0.54
161	42 49.9	91 59.0	360.6	980329.018	6.413	-33.953	-3.10	-2.16	-2.38	-1.93	-0.78	-1.18
162	42 50.0	92 0.1	353.9	980330.369	5.545	-34.070	-2.12	-0.81	-0.63	-0.17	0.83	-0.17
163	42 50.0	92 1.3	345.0	980333.671	6.119	-32.506	0.53	2.35	2.95	3.17	3.61	2.10
164	42 50.0	92 2.5	335.9	980332.282	1.909	-35.693	-1.56	0.88	1.91	1.49	1.06	-0.46
165	42 49.1	92 2.5	339.2	980331.781	3.793	-34.184	-0.34	1.39	1.87	0.26	-0.25	-1.33
166	42 49.1	92 1.3	338.0	980334.730	6.365	-31.475	1.27	2.41	2.44	1.65	1.91	0.30
167	42 49.1	92 0.1	346.3	980334.839	9.014	-29.748	1.89	2.56	2.17	1.80	2.56	1.17
168	42 49.0	91 59.0	350.5	980334.605	10.246	-28.993	1.55	1.86	1.08	0.86	1.73.	0.82
169	42 49.0	91 57.8	362.7	980333.713	13.116	-27.489	1.96	2.05	0.94	0.73	1.37	0.90

Sta. No.	Lat. North	Long. East	Elev. (meters)	Observed Gravity	Free Air Anomaly	Bouguer Anomaly	Residual Trend Surface					
							First	Second	Third	Fourth	Fifth	Sixth
170	42 49.0	91 56.6	348.1	980338.726	13.615	-25.352	3.00	2.97	1.54	1.28	1.43	1.22
171	42 48.2	91 56.6	343.8	980340.200	14.972	-23.517	4.53	3.77	1.98	1.40	1.47	0.96
172	42 48.1	91 57.7	351.1	980337.363	14.541	-24.767	4.38	3.68	2.14	1.50	1.94	1.19
173	42 48.1	91 58.9	333.1	980339.560	11.190	-26.104	4.13	3.62	2.37	1.60	2.22	1.12
174	42 48.1	92 0.1	341.4	980336.449	10.619	-27.597	3.73	3.53	2.62	1.53	2.07	0.68
175	42 48.1	92 1.3	359.1	980337.033	(erroneous values--not employed in mapping)							
176	42 48.1	92 2.5	340.2	980331.482	5.275	-32.805	0.71	1.51	1.43	-1.35	-1.79	-1.81
177	42 47.3	92 2.4	325.2	980336.048	6.433	-29.975	3.21	2.96	2.45	-1.01	-1.27	0.04
178	42 47.3	92 1.3	319.1	980338.983	7.487	-28.238	3.85	3.07	2.15	-0.04	0.05	-0.43
179	42 47.3	92 0.1	332.8	980337.570	10.306	-26.955	4.04	2.87	1.60	0.18	0.50	-0.48
180	42 47.3	91 58.9	351.7	980335.466	14.033	-25.343	4.57	3.13	1.57	0.60	0.95	0.06
181	42 47.3	91 57.7	350.5	980337.665	15.856	-23.384	5.44	3.85	2.06	1.31	1.53	0.90
182	42 47.2	91 56.5	360.3	980336.766	18.116	-22.216	5.52	3.87	1.92	1.29	1.28	0.83
183	42 53.4	91 48.5	342.0	980343.911	10.320	-27.965	-5.59	-2.83	-3.66	-2.03	-1.23	-1.66
184	42 53.0	91 47.9	335.3	980344.711	9.651	-27.883	-6.21	-2.94	-4.13	-2.03	-0.87	-1.02
185	42 52.4	91 47.1	346.9	980341.784	11.197	-27.633	-6.91	-2.95	-4.51	-2.03	-0.25	-0.10
186	42 52.0	91 46.5	337.1	980343.421	10.425	-27.313	-7.28	-2.82	-4.57	-2.08	-0.09	0.25
187	42 51.5	91 46.0	287.1	980353.031	5.361	-26.782	-7.46	-2.47	-4.31	-2.09	-0.08	0.37
188	42 51.0	91 45.4	353.0	980341.422	14.816	-24.697	-6.00	-0.57	-2.38	-0.76	0.80	1.27
189	42 50.0	91 44.2	351.1	980347.011	21.340	-17.968	-0.79	5.69	4.53	3.18	1.36	1.29
190	42 49.5	91 43.6	298.1	980359.267	17.982	-15.388	1.12	8.08	7.47	4.07	-0.75	-1.44
191	42 46.4	92 2.4	315.5	980338.240	6.965	-28.351	4.51	3.02	2.20	-1.34	-1.52	1.27
192	42 46.4	92 1.2	331.0	980335.941	9.462	-27.594	4.17	2.17	1.00	-1.09	-1.28	-0.79
193	42 46.4	92 0.1	331.0	980337.282	10.803	-26.253	4.42	2.06	0.60	-0.56	-0.75	-1.03

Sta. No.	Lat. North	Long. East	Elev. (meters)	Observed Gravity	Free Air Anomaly	Bouguer Anomaly	Residual Trend Surfaces					
							First	Second	Third	Fourth	Fifth	Sixth
194	42 46.4	91 58.9	340.5	980336.989	13.426	-24.688	4.90	2.29	0.61	0.01	-0.22	-0.54
195	42 46.4	91 57.7	351.1	980337.035	16.763	-22.545	5.95	3.21	1.39	1.10	0.80	0.67
196	42 46.4	91 56.5	354.5	980337.626	18.389	-21.294	6.11	3.38	1.49	1.35	1.01	1.03
197	42 45.5	91 56.5	340.5	980339.606	17.392	-20.722	6.37	2.39	0.87	2.02	0.70	1.36
198	42 45.5	91 57.7	342.0	980337.415	15.671	-22.613	5.57	1.60	0.01	0.98	-0.46	-0.03
199	42 45.5	91 58.9	335.3	980336.772	12.959	-24.575	4.70	0.80	-0.74	-0.10	-1.54	-1.38
200	42 45.5	91 60.0	335.0	980335.431	11.524	-25.976	4.36	0.65	-0.77	-0.72	-2.03	-1.89
201	42 45.5	92 1.2	321.6	980337.330	9.285	-26.713	4.74	1.35	0.14	-0.86	-1.88	-0.93
202	42 45.5	92 2.4	324.9	980335.875	8.865	-27.508	5.04	2.16	1.24	-1.42	-1.93	1.56
203	42 58.8	92 3.7	326.1	980346.014	- 0.569	-37.079	1.13	2.87	-0.06	-1.08	-1.61	-0.82
204	42 59.4	92 2.5	316.4	980351.911	1.419	-33.999	3.34	3.26	-0.41	-0.57	-2.37	-1.48
205	42 60.0	92 1.3	310.0	980358.551	5.183	-29.518	6.93	5.03	0.59	1.38	0.45	0.64
206	42 0.5	92 0.7	330.1	980354.730			(erroneous values--not employed in mapping)					
207	42 58.7	91 48.3	357.2	980353.731	16.891	-23.100	0.83	-1.27	-0.56	0.12	-0.60	0.34
208	42 58.7	91 49.5	367.3	980350.671	16.935	-24.182	0.87	-1.72	-0.82	-1.17	-2.25	-0.87
209	42 58.7	91 50.7	356.3	980353.124	16.002	-23.886	2.26	-0.66	0.36	-0.85	-1.87	-0.46
210	42 58.7	91 51.8	370.0	980350.113	17.223	-24.200	3.05	-0.05	1.03	-0.84	-1.56	-0.44
211	42 58.7	91 53.0	359.1	980351.199	14.923	-25.272	3.07	-0.08	1.00	-1.25	-1.61	-0.96
212	42 58.7	91 54.2	350.5	980350.655	11.746	-27.494	1.94	-1.18	-0.18	-2.50	-2.59	-2.41
213	42 58.7	91 55.7	352.0	980348.897	10.458	-28.952	1.84	-1.02	-0.20	-2.26	-2.38	-2.70
214	42 58.7	91 57.2	341.1	980352.131	10.307	-27.875	4.00	1.47	2.02	0.42	-0.09	-0.59
215	42 58.7	91 58.1	342.0	980351.704	10.162	-28.123	5.69	4.02	3.89	3.31	1.42	1.11
216	42 58.7	92 0.1	329.8	980354.719	9.414	-27.505	7.41	6.42	5.76	5.67	2.89	·2.93

| Sta. No.	Lat. North	Long. East	Elev. (meters)	Observed Gravity	Free Air Anomaly	Bouguer Anomaly	Residual Trend Surfaces					
							First	Second	Third	Fourth	Fifth	Sixth
217	42 58.8	92 1.4	334.7	980349.857	5.907	-31.558	4.46	4.24	2.91	3.05	-0.22	0.21
218	42 58.8	92 2.5	336.2	980345.223	1.744	-35.892	1.21	1.90	-0.15	-0.24	-3.04	-2.31
219	42 59.6	92 1.4	313.3	980356.859	5.126	-29.951	6.35	5.09	1.84	2.22	0.00	0.41
220	42 59.6	92 0.1	313.9	980358.427	6.882	-28.263	6.94	4.83	2.42	2.80	0.88	0.84
221	42 59.6	91 59.0	334.7	980354.246	9.097	-28.369	5.74	2.96	1.28	1.37	0.25	-0.06
222	42 59.6	91 57.1	326.4	980355.334	7.645	-28.899	3.52	-0.07	-0.85	-1.41	-1.23	-1.47
223	42 59.6	91 55.7	333.5	980353.794	8.267	-29.061	2.00	-2.06	-2.31	-3.26	-2.49	-2.25
224	42 59.6	91 54.5	355.1	980350.193	11.344	-28.407	1.59	-2.71	-2.66	-3.70	-2.90	-2.11
225	42 59.6	91 53.0	356.0	980352.774	14.208	-25.646	2.99	-1.42	-1.08	-1.94	-1.59	-0.14
226	42 59.6	91 51.8	347.5	980356.653	15.453	-23.445	4.08	-0.30	0.15	-0.19	-0.46	1.33
227	42 59.6	91 50.7	371.9	980352.302	18.625	-23.003	3.43	-0.79	-0.31	0.13	-0.84	0.87
228	42 59.6	91 49.5	368.2	980353.283	18.478	-22.741	2.60	-1.34	-0.89	0.55	-1.06	-0.01
229	42 59.6	91 48.3	369.7	980353.490	19.155	-22.234	2.00	-1.52	-1.17	1.45	-0.61	-0.94
230	43 0.5	91 48.3	374.3	980355.490	21.216	-20.686	3.83	-1.22	-1.52	4.36	1.48	-3.26
231	43 0.4	91 49.5	373.4	980355.231	20.825	-20.974	4.65	-0.81	-1.12	3.49	2.07	0.26
232	43 0.4	91 51.3	338.6	980361.776	16.648	-21.260	6.02	0.16	-0.36	2.74	3.55	4.03
233	43 0.4	91 53.0	339.9	980356.924	12.173	-25.872	3.04	-2.84	-3.67	-1.78	0.66	1.72
234	43 0.4	91 54.4	303.0	980362.090	5.959	-27.958	2.23	-3.52	-4.79	-3.31	-0.10	0.54
235	43 0.5	91 55.8	338.0	980353.746	8.280	-29.560	2.04	-3.37	-5.28	-3.90	-0.57	-0.67
236	43 0.4	91 57.1	306.6	980359.753	4.751	-29.575	3.12	-1.87	-4.40	-2.92	-0.07	-0.68
237	43 0.5	91 58.6	328.9	980355.979	7.692	-29.125	4.96	0.68	-2.80	-1.12	0.70	-0.22
238	43 0.4	92 0.1	336.2	980353.800	7.920	-29.716	5.76	2.41	-2.20	-0.50	0.34	-0.38
239	43 0.5	92 1.4	315.5	980357.799	5.374	-29.942	6.64	4.10	-1.63	-0.20	0.76	0.47
240	43 0.5	92 2.5	330.4	980352.972	5.155	-31.833	5.84	4.25	-2.72	-2.09	0.37	0.70
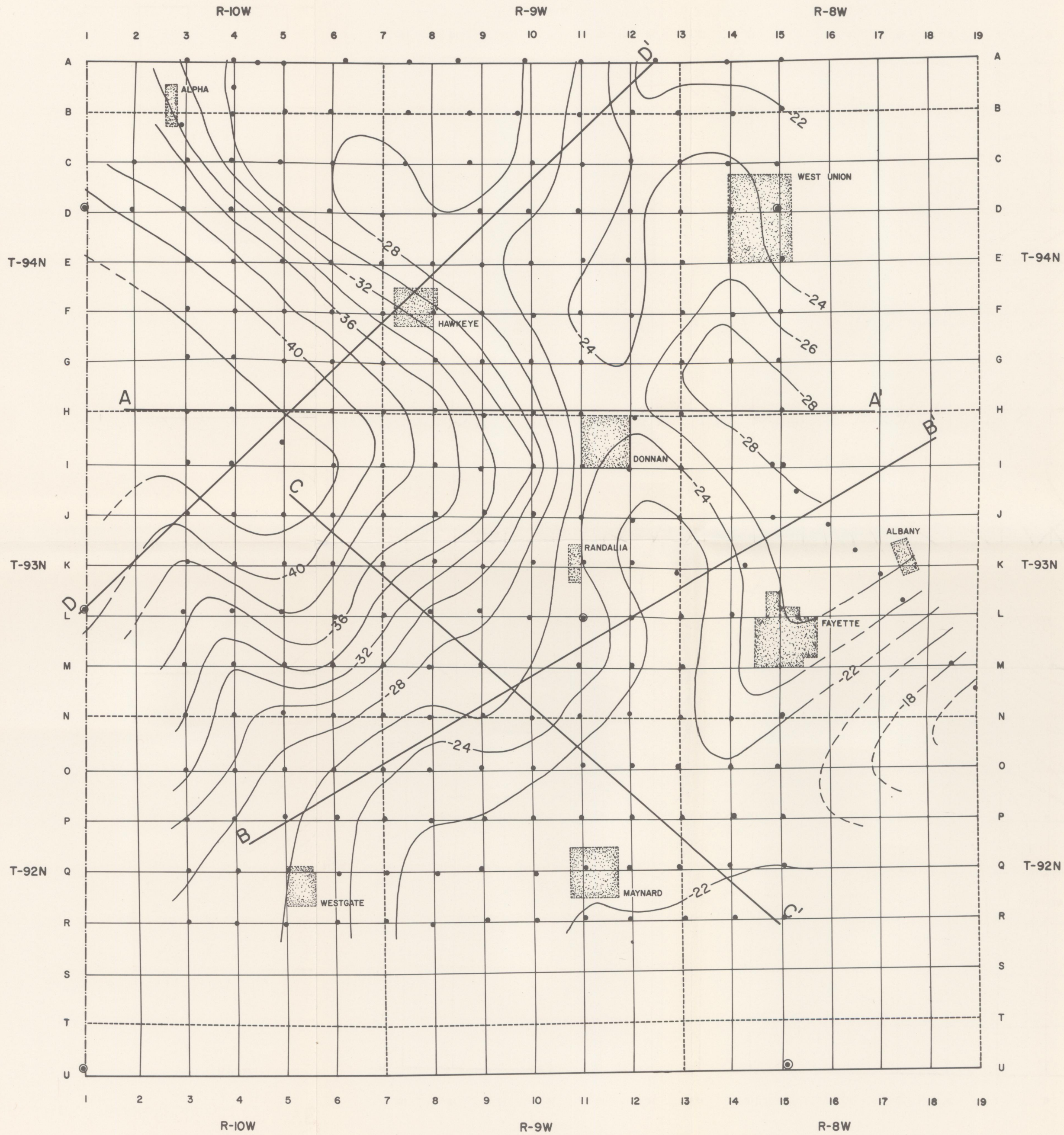
BOUGUER GRAVITY MAP

LEGEND

⊙   Gravity Base Station

•   Gravity Observation Station

—-24—   Isogal

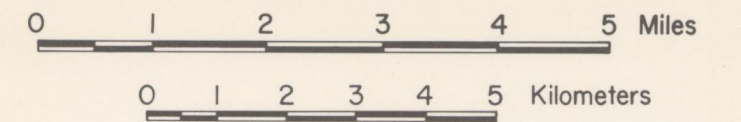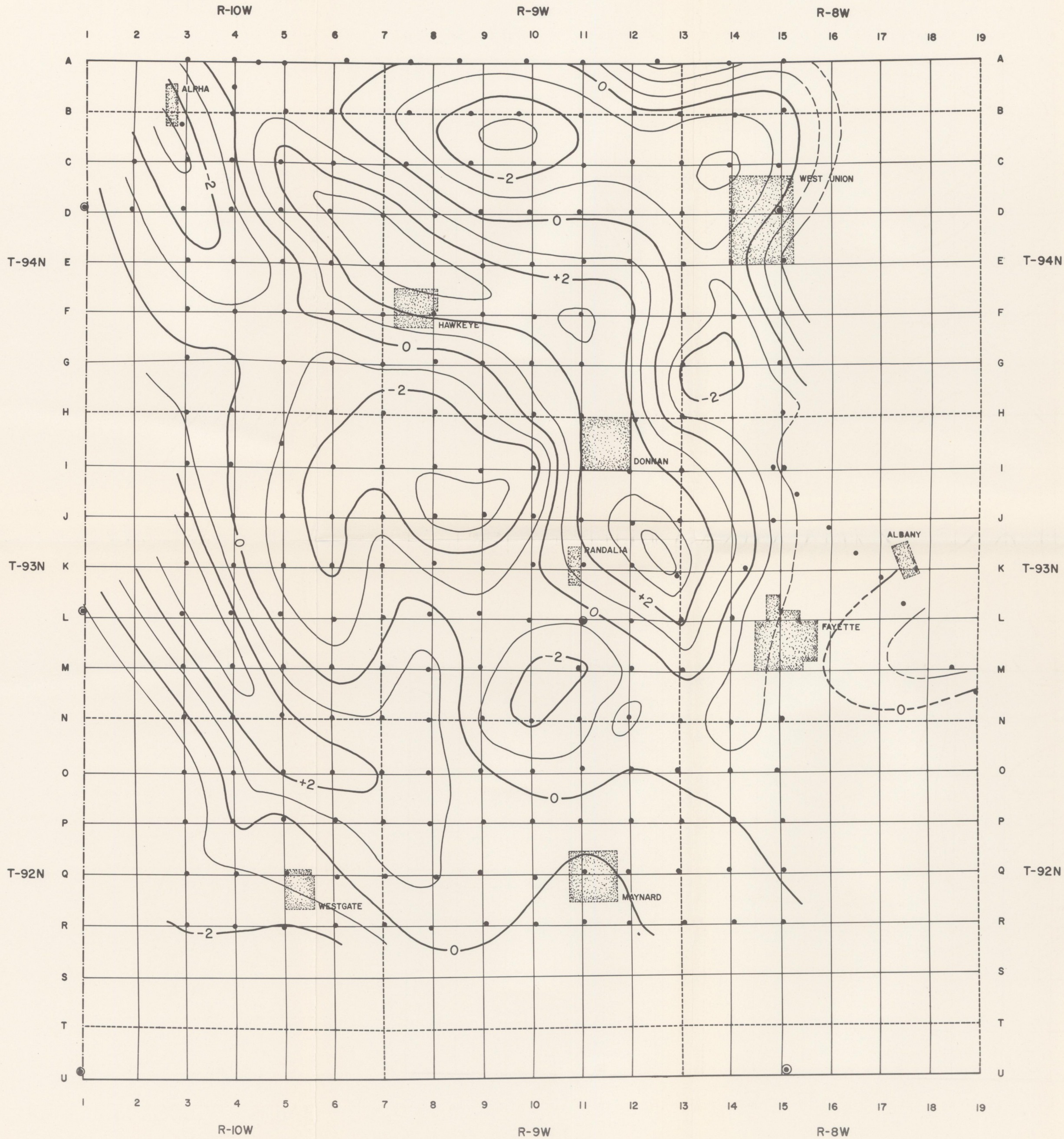Contour Interval 2 mgal

A ——— A'   Gravity and Magnetic Profile
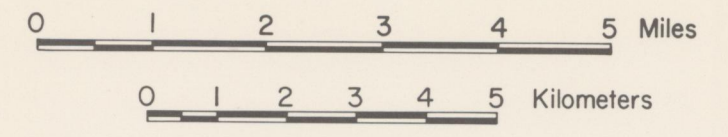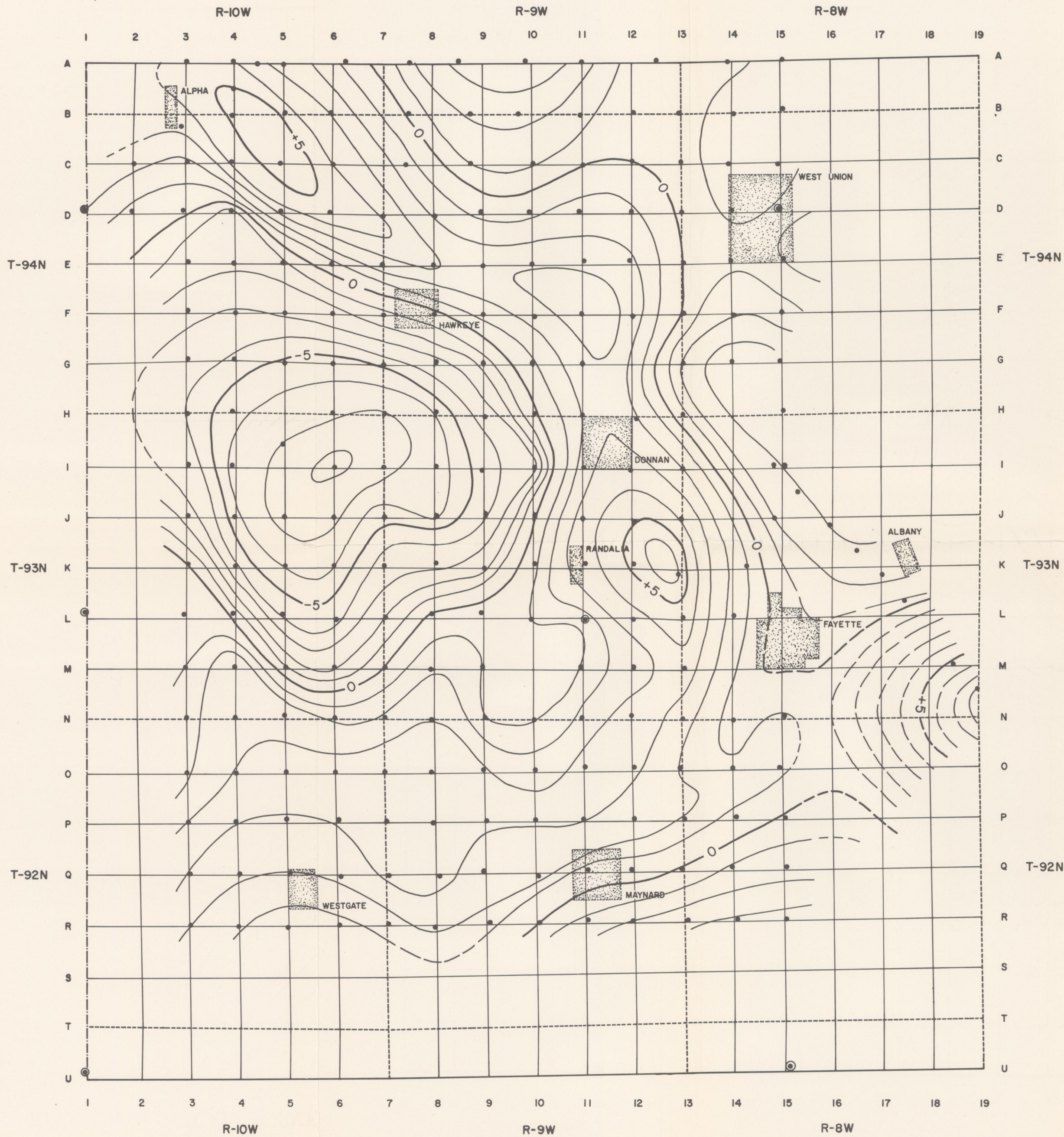
SECOND DEGREE RESIDUAL
GRAVITY MAP

LEGEND

◉ Gravity Base Station

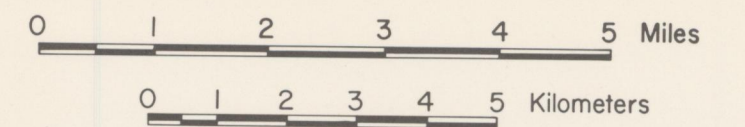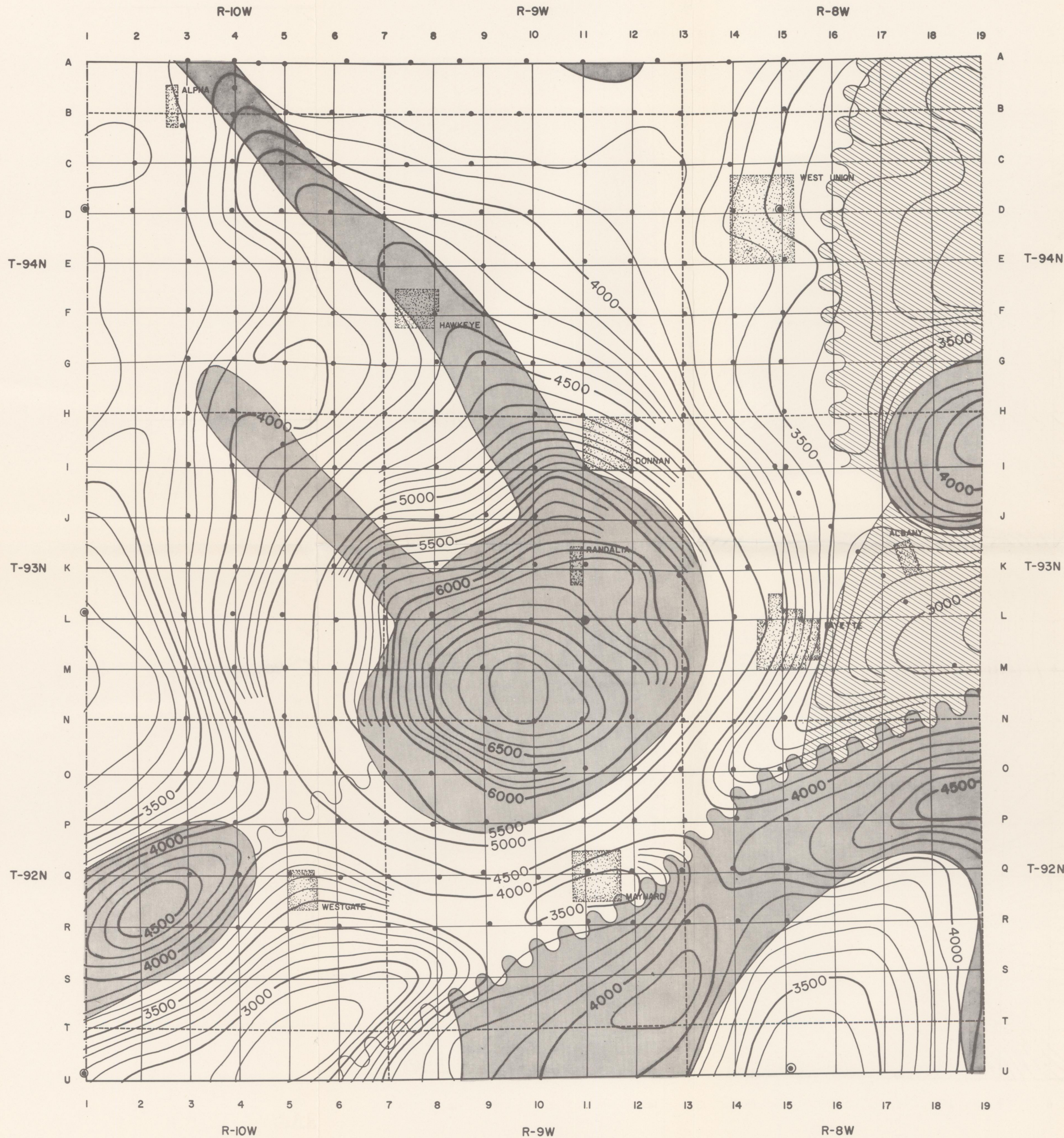• Gravity Observation Station

⌐+5⌐ Isogal

Contour Interval 1.0 mgal

R-10W   R-9W   R-8W

T-94N   T-93N   T-92N

ALPHA   WEST UNION   HAWKEYE   DONNAN   RANDALIA   ALBANY   FAYETTE   WESTGATE   MAYNARD

0 1 2 3 4 5 Miles

0 1 2 3 4 5 Kilometers

FIFTH DEGREE RESIDUAL
GRAVITY MAP

LEGEND

⊙   Gravity Base Station

•   Gravity Observation Station
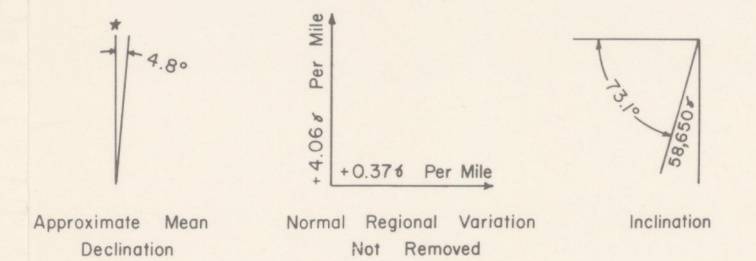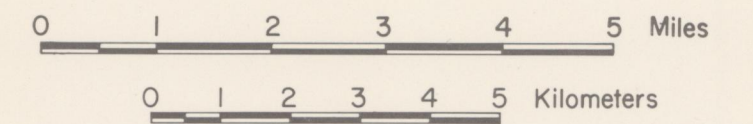
—+2—   Isogal
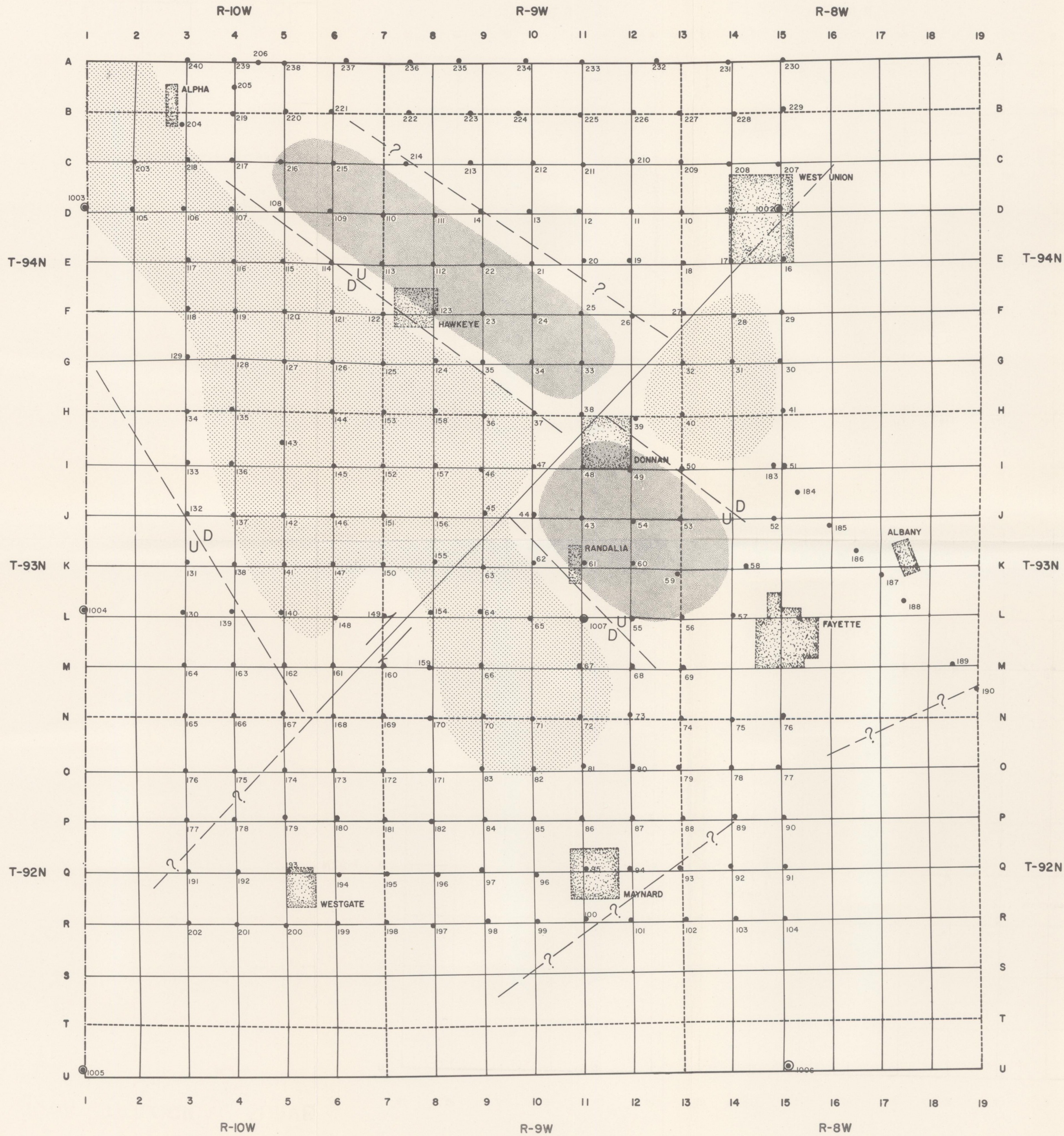
Contour Interval 1.0 mgal

AEROMAGNETIC   MAP
AND
GEOPHYSICAL   INTERPRETATION
OF
BASEMENT   COMPLEX

LEGEND

- Acidic Composition
- Intermediate Composition
- Basic Composition
- Probable Fault
- Gravity Base Station
- Gravity Observation Station

Flight Altitude 1000 Ft. T.C.

Flight Interval 1 Mile

Base Intensity Arbitrary

Contour Interval 20 Gammas

0 1 2 3 4 5 Miles

0 1 2 3 4 5 Kilometers

Approximate Mean
Declination

Normal Regional Variation
Not Removed

Inclination

GEOPHYSICAL INTERPRETATION
OF
GRAVITY SURVEY

LEGEND

⊙ 1007 Gravity Base Station

• 195 Gravity Observation Station

U/D Proposed Basement Fault

Possible Thick PreCambrian (?) Clastic Deposits

Basic Intrusive Bodies

0 1 2 3 4 5 Miles

0 1 2 3 4 5 Kilometers